ICES
CIEM

International Council for the Exploration of the Sea

Conseil International pour l'Exploration de la Mer

Demersal fish and invertebrate catches relative to construction and operation of North America's first offshore wind farm

Dara H. Wilber[1,*], Lorraine Brown[1,2], Matthew Griffin[1,3], Gregory R. DeCelles[4] and Drew A. Carey[1]

[1]INSPIRE Environmental, Newport, RI, USA
[2]Exa Data and Mapping, Poulsbo, WA, USA
[3]Saltbox Sea Farm, North Kingstown, RI, USA
[4]Orsted Offshore North America, Providence, RI, USA

*Corresponding author: Tel: +1 843 469 6961; E-mail: dara@inspireenvironmental.com

Effects of offshore wind farm (OSW) development in the US on fishery resources have been predicted based on European experience. A seven-year study of the first US OSW documented the response of demersal fish and invertebrates to construction and operation. Local fishermen and scientists designed a monthly demersal trawl survey using a Before-After-Control-Impact (BACI) design to assess potential effects of Block Island Wind Farm (BIWF), a pilot scale 30 MW project completed in 2016. Common species did not exhibit statistically significant ($\alpha = 0.10$) BACI interactions in catch per unit effort (CPUE) due to BIWF operation. CPUE of structure-oriented species, such as black sea bass (*Centropristis striata*) and Atlantic cod (*Gadus morhua*), increased at BIWF following turbine installation. Fall and spring biomass varied synchronously between BIWF and a regional survey for several species including longfin squid (*Loligo pealeii*) and winter flounder (*Pseudopleuronectes americanus*). Spatial-temporal interaction between reference areas provided an estimate of the minimum effect sizes (approximately 40% to 63% among the fish evaluated) that may be considered ecologically significant when assessing potential OSW impacts. Results from this first North American OSW fisheries monitoring study provide valuable information for future OSW development on the northeastern US coastline.

Keywords: Block Island Wind Farm, renewable energy, environmental impact assessment, Before-After Control-Impact, trawl survey.

Introduction

Offshore wind energy has been an alternative to carbon emitting energy sources on a commercial scale in Europe since 2002 (Bailey *et al.*, 2014) and offshore wind development began in 2009 on the northeastern coast of the US. Multiple studies have evaluated the effects of European wind farms on fishery resources (e.g. Leonard *et al.*, 2011; Degraer *et al.*, 2012; van Deurs *et al.*, 2012; Bergstrom *et al.*, 2013; Vandendriessche *et al.*, 2015; Langhamer *et al.*, 2016). In the US, assessments of potential effects of wind farm development on fish and invertebrates include pre-development surveys (Walsh and Guida, 2017; Secor *et al.*, 2020) and predictive consideration of effects to long-established commercial fishing industries (Lipsky *et al.*, 2016; NASEM, 2017). European studies have found minor to moderate effects from wind farm construction and operation on fish and invertebrate communities, however, the relevance of these studies to predicting potential effects on the northeastern US coast is complicated by the differences in biological communities and smaller scale of currently operating US wind farms. European reviews of wind farm effects emphasize the need for sampling fish and invertebrate communities before, during, and after construction (Lindeboom *et al.*, 2011; Vandendriessche *et al.*, 2015). Potential changes to fish and invertebrate communities include an attraction to the introduced structure (e.g. Maar *et al.*, 2009; Andersson and Ohman, 2010; Reubens *et al.*, 2013a), as occurs at artificial reefs and oil platforms (e.g. Wolfson *et al.*, 1979; Harrison and Rousseau, 2020). Potential negative impacts include responses to noise (Wahlberg and Westerberg, 2005; Popper and Hawkins, 2019; Tougaard *et al.*, 2020) and electromagnetic fields (EMF; Taormina *et al.*, 2018; Hutchison *et al.*, 2020) that may elicit avoidance behaviors or stress that could affect reproduction and trophic interactions. It is important, therefore, to document demersal fish and invertebrate responses to wind farm construction and operation in the US to anticipate and minimize potential impacts as offshore wind development expands.

North America's first offshore wind farm (OSW), Block Island Wind Farm (BIWF) began operation in October, 2016. It is located approximately 5 km southeast of Block Island, Rhode Island in an area that was historically fished by commercial trawl, gillnet, and lobster vessels, as well as the recreational fishing community (Lipsky *et al.*, 2016). Built on a pilot scale, it consists of five, 6 MW wind turbine generators (Figure 1), with steel jacket foundations. The overall turbine height is 150 m and the footprint of each foundation is approximately 576 m². Construction effects on the physical environment were monitored to establish recovery from alterations to benthic habitats (Guarinello and Carey, 2020) and sediment suspension during cable installation, which were minor (Elliot *et al.*, 2017). Effects of construction and operation of BIWF on demersal fish and invertebrates were a primary concern for those highly dependent on commercial and recreational fishing in the area. Discussions between wind energy representatives and fishing communities over several years resulted in a collaborative study using commercial fishing ves-
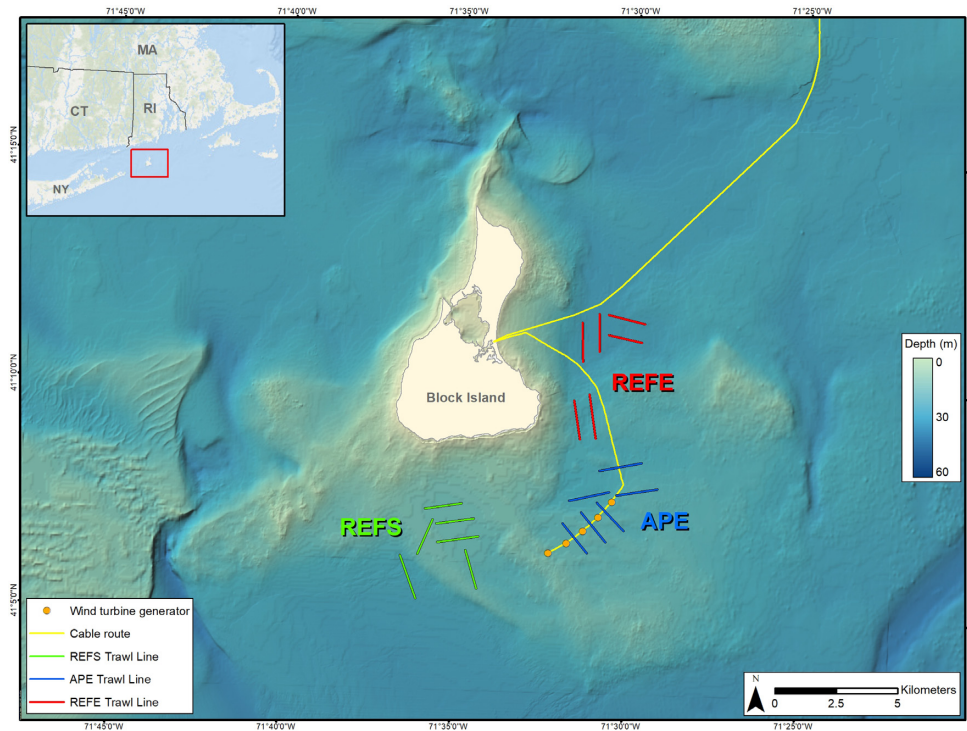
Figure 1. Block Island Wind Farm demersal fish trawl study area with the locations of the six fixed trawl lines in each survey area; the Area of Potential Effect (APE), Reference Area South (REFS), and Reference Area East (REFE).

sels and gear to provide data on the seasonal abundances of fish and invertebrates at the BIWF during baseline, construction and operation time periods (INSPIRE, 2021). The resultant demersal trawl survey was conducted over seven years (2012–2019) using a Before-After Control-Impact (BACI) study design (Underwood, 1992; Smith *et al.*, 1993). This study approach has been used to compare fish communities between wind farm and reference areas in Europe using a variety of sampling gears, e.g. beam trawl (Lindeboom *et al.*, 2011; Vandendriessche *et al.*, 2015; Degraer *et al.*, 2018), fyke nets (Bergstrom *et al.*, 2013), and gill nets (Stenberg *et al.*, 2015). Reference site locations are typically chosen based on physical characteristics, such as water depth and bottom type, that are similar to the impact area. The BIWF bottom trawl survey builds upon comprehensive trawl sampling conducted in Block Island Sound and Rhode Island Sound that documented strong seasonal variation and persistent interannual fish assemblage structure (Malek *et al.*, 2014; Guida *et al.*, 2017).

In addition to examining potential BIWF construction and operation effects on demersal fish and invertebrate communities, examination of observed temporal changes in catch per unit effort (CPUE) between reference areas provides a basis for assessing target effect sizes. The magnitudes of spatial-temporal interaction between the two reference areas are summarized for select species, providing an example of the level of change that may be reasonable to target when planning future OSW monitoring studies of these fish and invertebrate species, based on the sampling design and modeling approach used in this study. High variance is common in abundance data collected from bottom trawl surveys (Smith, 1996) and sampling with a trawl net, which has the potential for large catches because gear saturation rarely occurs, can also exacerbate variability in monitoring data. Frequently, fish and invertebrate catch data are highly skewed due to a few, very large catches

(Smith, 1996; Frisk *et al.*, 2011; Sagarese *et al.*, 2015) that may result from patchy distributions related to temperature preferences, density-dependent habitat selection, and small-scale aggregations (Blanchard *et al.*, 2008). The challenge for fisheries monitoring studies intended to measure effects from OSW development is to first determine biologically meaningful effect sizes and then design the study to characterize this level of change with sufficient statistical power or precision. These biologically meaningful effect sizes are often defined through public policy or extensive basic research and target effect sizes have not yet been established for fish and invertebrates in relation to offshore infrastructure in the US. The analyses in this study provide estimates of the magnitude of effects observed, with confidence intervals, which will be helpful in advancing the science in support of sound policy that manages the effects of an emerging offshore wind industry on the northeastern US coast.

Methods

Study area

The BIWF demersal trawl survey was conducted within the wind farm construction footprint, hereafter referred to as the Area of Potential Effect (APE), and in two reference areas that have similar habitat characteristics (Figure 1). Benthic assessments of sampling areas were conducted using multibeam bathymetry, video, and still imagery to determine habitat characteristics adjacent to the wind farm (LaFrance, *et al.*, 2010; Guarinello and Carey, 2020) and reference areas. Tow lines in the APE were arranged N-S and E-W around and across the wind turbine generator area and inter-array cables at depths ranging from 24 to 30 m over primarily silty sand, sand, and gravel. The Reference Area South (REFS) is located south of

Block Island and west of the APE, separated by a ridge of glacial moraine (till, boulders, and cobbles), with tow lines at depths from 18 to 37 m over primarily sand and gravel. The Reference Area East (REFE) is located east of Block Island and north of the APE, with tow lines at 24 to 40 m depths over primarily silty sand and silt (Figure 1).

Trawl survey

Demersal fish and invertebrates were surveyed monthly from October 2012 to September 2019 using the same commercial fishing vessel (FV Virginia Marise), captain, and crew, with scientists onboard to process the catch. Each month, two replicate, 20-min tows were conducted in each reference area and in the APE, resulting in six tows per month (Figure 1). Tows in each area were randomly selected from six pre-determined, fixed tow lines known to be accessible for trawling (based on captain's experience), but subject to seasonal location of fixed fishing gear (e.g. gill nets and lobster trawls). On occasion, tow line selection was adjusted to account for field conditions (e.g. prevailing wind, tidal currents, known obstructions and hang ups, and fixed fishing gear). Towing was conducted during the day using a 412×12 cm, four-seam whiting trawl with 168-cm Thyburon otter doors and a 2.54 cm knotless cod end liner to ensure retention of the smaller fish. This gear is the same trawl net used by the Northeast Area Monitoring and Assessment Program (NEAMAP) bottom trawl survey (Bonzek *et al.*, 2017) and is similar to the National Oceanic and Atmospheric Administration (NOAA) Fisheries Northeast Fisheries Science Center (NEFSC) bottom trawl survey net (NEFSC, 2018) to allow comparability of results. The NEAMAP survey is conducted from Cape Hatteras, NC to Cape Cod, MA and overlaps the federal and many state surveys.

Fish collected in each tow were identified, weighed, and enumerated consistent with the sampling approach of the NEAMAP survey plan. In the case of larger catches (e.g. > 900 kg), subsampling procedures were used (Bonzek *et al.*, 2017). Following each tow, size measurements (mm) were recorded for 50 individuals of each species and stomachs were sampled for select species. Length frequency distributions (IN-SPIRE, 2021) and dietary analyses (Wilber *et al.* 2022) are addressed elsewhere. Bottom water temperature, dissolved oxygen (DO), and salinity data were collected at the end of each tow using a YSI model 6820 V2 water quality meter.

Data analyses

Seasons were defined based on monthly groupings with similar bottom water temperature variation. Fall includes months with decreasing water temperatures (October through December), winter extends from January through April, spring includes May through July, and summer includes August and September. Time periods are defined as: baseline (October 2012 through September 2014), construction phase I (July 2015 through October 2015), construction phase II (April 2016 through September 2016), and operation (October 2016 through September 2019). Separate models were constructed for each impact phase, and the months for "baseline" periods included October–September (baseline versus operation), July–October (baseline versus construction phase I), and April–September (baseline versus construction phase II). Multiple disturbances occurred during each phase of construction, but broadly described; construction phase I includes wind turbine foundation construction and installation (e.g. pile driv-

ing), and construction phase II includes cable installation and turbine construction (e.g. turbine and blade installation, jet plow trenching).

Generalized Linear Models (GLM)

A negative binomial GLM with a log-link was used to model the species catch data. The log-link accounts for multiplicative effects on catch, and the negative binomial is appropriate for overdispersed count data (e.g. ver Hoef and Boveng, 2007; Lindén and Mäntyniemi, 2011). Total monthly catch (number) was the response variable, using the number of tows per month as an offset in the model, effectively modeling catch per tow (CPUE). Overdispersion was observed in the residual plots, and the appropriateness of the negative binomial over a Poisson distribution was tested with a likelihood ratio test using *odTest* in the *pscl* package (Jackman, 2020) in R (R Core Team, 2020). Models considered fixed categorical covariates of Area (APE, REFS, and REFE) crossed with Period (Baseline and Operation), crossed with Season (four levels, described above). The possible continuous environmental covariates included water depth, bottom water temperature and bottom dissolved oxygen (DO).

Initial model selection for each species was conducted using forward and backward stepwise elimination using the *stepAIC* function in the MASS package (Venables and Ripley, 2002), with the lower bound for models set to Area∗Period, and the upper bound set to Area∗Period∗Season plus linear (depth, temperature, and DO), quadratic (temperature and DO), or polynomial (linear + quadratic for temperature and DO) effects of the continuous covariates. Both temperature and DO covariates were centered on the mean prior to inclusion in the model to remove collinearity between these variables and their squares. The models selected by *stepAIC* were evaluated further for multicollinearity (assessed using car::vif), and if elevated, alternative models were sought. The final selection was the most parsimonious model with the best fit, including the lowest Akaike Information Criterion corrected for small sample sizes (AICc, Burnham and Anderson, 2002) by a minimum delta of 2, and the best residuals based on a visual evaluation of the diagnostic plots for homogeneity and balance. Serial correlation was tested with a Durbin–Watson test [*dwtest* in the *lmtest* package, Zeileis and Hothorn, 2002] within each area and period.

The GLMs estimated the number of individuals for a species caught by area, season, and period. A model including two-way interactions between the fixed factors plus a polynomial (linear and quadratic) temperature effect is illustrated in [Eq. 1].

$$Catch_{apsm} \sim NegBinomial\left(\mu_{apsm},\ \kappa\right)$$

$$E[Catch_{apsm}] = \mu_{apsm} \quad \text{and}$$

$$Var[?Catch_{apsm}] = \mu_{apsm} + \kappa\mu_{apsm}^2$$

$$\log\left(\mu_{apsm}\right) = Area_a + Area_a : Period_p + Season_s$$
$$+ Area_a : Season_s + Period_p : Season_s$$
$$+ \beta_1 T_{apsm} + \beta_2 T_{apsm}^2, \tag{1}$$

where $Catch_{apsm}$ is the mth observation for the number of individuals for a species caught across all tows in Area a ($a = 1$ to 3 for APE, REFE, and REFS), period p ($p =$ Baseline or Operation), and season s ($s =$ Fall, Winter, Spring, Summer),

where $m = 1$ to the total number of months x years in each Area-Period-Season. T_{apsm} is the average temperature from the two tows associated with observation m, area a, period p, season s, centered on the mean. The log (number of tows) is included as an offset (note: there were two tows per month on all but three occasions when only a single tow was successful), hence the model effectively estimates catch per tow (CPUE). Results for each species model are presented in Supplementary Appendix S1.

Linear Contrasts and their 90% Confidence Intervals

From each of the final models, linear contrasts were constructed to estimate differences in CPUE between time periods within each area (temporal change), between areas within each period (spatial change), and the BACI interaction (differences between reference and APE temporal changes, or equivalently, differences between baseline and operation spatial changes). The term "BACI interaction" is used as a shorthand descriptor of the complex contrast estimated from the GLM (Seltman, 2018; Schad *et al.*, 2020), and does not refer to the simple area x period interaction from a two-factor ANOVA. When environmental variables were present in a final model, it meant that CPUE trends could partially be explained by these variables. In order to isolate area and period differences, the CPUE estimates from these models were standardized to a common set of values for any environmental covariates in the model. Contrasts were calculated as linear differences on the log-scale (the scale in which the model was fit), which equates to proportional change (ratios) on the original measurement scale. Representing changes in CPUE as proportional rather than linear on the measurement scale is an effective way to compare changes across different groups that might have widely different baseline values. The BACI contrast is the proportional temporal change at a reference area expressed as a % of the proportional temporal change at the APE:

$$BACI\ as\ \%\ change = \left(\frac{CPUE_{REF,Operation}/CPUE_{REF,Baseline}}{CPUE_{APE,Operation}/CPUE_{APE,Baseline}} - 1 \right) x100. \tag{2}$$

For example, if the baseline and operation mean CPUE values were 200 and 80, respectively, for a reference area, and 100 and 60 for the APE, then the BACI contrast would be estimated as $[(80/200)/(60/100) -1] = (0.40/0.60-1) = (0.67-1) = -0.33$, indicating a 33% lower temporal ratio at the reference than at the APE. Negative values reflect either a bigger increase, or a smaller decrease in CPUE between time periods at the APE, whereas positive values reflect the reverse situation, i.e. a smaller increase, or bigger decrease in CPUE at the APE. The expected value and the 90% confidence interval (90CI) for each contrast were based on a simulated distribution of linear contrast estimates, derived using Monte Carlo methods drawing from the multivariate distribution of GLM coefficients (e.g. Tofighi and MacKinnon, 2016). The contrast and its 90CI were the inverse-log (exponential) of the median, and the 5th and 95th percentiles, respectively, of the simulated distribution of each linear contrast estimated from the GLM (with a log-link function). The 90CI provides information about magnitude and precision of the estimated contrast, with wide CIs indicative of large variance or outliers in the underlying data. If the 90CI excludes zero, the interaction is statistically significant (two-tailed $\alpha = 0.10$). A 90% confidence level was used to provide a high level of confidence for the estimated effects without overly restricting the power of the tests, i.e. the probability of identifying a statistically significant effect of wind farm operation.

Operation Effects

Potential impacts of wind farm operation on fish and invertebrate CPUE were evaluated using GLMs (Eq. 1), for the baseline (September 2012–October 2014) and operation (September 2015–October 2019) time periods. The factors included in each final model varied by species (see Supplementary Appendix S1). The GLMs were fit for the species that were frequently caught in the survey: black sea bass (*Centropristis striata*), little skate (*Leucoraja erinacea*), summer flounder (*Paralichthys dentatus*), windowpane (*Scophthalmus aquosus*), winter flounder (*Pseudopleuronectes americanus*), winter skate (*Leucoraja ocellata*), and longfin squid (*Loligo pealeii*).

Because a potential wind farm effect on fish includes changes to prey availability (Lindeboom *et al.*, 2011) and diet composition (Reubens *et al.*, 2013b), multivariate analyses were conducted to determine whether either benthivore and piscivore assemblages differed by area, time period, or an interaction of these factors. Trophic categories were based on dietary guild identifications and stable isotope analysis for the fish community in Rhode Island and Block Island Sounds (Malek *et al.*, 2016). Planktivores and crustacivores also were identified by Malek *et al.* (2016), but low sample sizes for fish in these trophic categories made them less suitable for multivariate analyses. Benthivores collected in the BIWF survey include scup (*Stenotomus chrysops*), winter flounder, little skate, winter skate, Atlantic herring (*Clupea harengus*), yellowtail flounder (*Limanda ferruginea*), and haddock (*Melanogrammus aeglefinus*); whereas piscivores include weakfish (*Cynoscion regalis*), striped bass (*Morone saxatilis*), summer flounder, spiny dogfish (*Squalus acanthias*), bluefish (*Pomatomus saltatrix*), monkfish (*Lophius americanus*), and silver hake (*Merluccius bilinearis*). Although not examined in Malek *et al.* (2016), the northern sea robin (*Prionotus carolinus*) was included in the benthivore group because in latter years, it was among the numerically dominant species in the BIWF survey. Two-way permutational multivariate analysis of variance (PERMANOVA; Anderson *et al.*, 2008) tests were conducted separately on each trophic group by season using Bray-Curtis dissimilarity measures created from CPUE data that were log transformed to increase the contribution of the less abundant species to the analyses (Clarke *et al.*, 2014). For each term in the model, 9999 permutations of the data were computed to obtain p-values. Similarity Percentage (SIMPER) analyses were conducted to determine the taxa contributing at least 5% to observed dissimilarities either between time periods or among areas and data for the analyses with strong dissimilarities were visualized using non-metric multidimensional scaling (nMDS) plots. On these plots, symbols spaced in close proximity to each other reflect similar taxonomic composition of the mean monthly samples, whereas more distantly spaced symbols reflect dissimilar assemblage composition. For each plot, the stress value represents a measure of the goodness-of-fit of the nMDS ordination. Stress values < 0.05 give an excellent representation of the data, < 0.1 corresponds to a good ordination, and < 0.2 give a potentially useful two-dimensional representation, but for values at the upper end of this range, little reliance should be placed upon the plot (Clarke *et al.*, 2014).

Construction Effects

To address the potential effects of construction activities, GLM analyses similar to those described above for assessing operation effects were conducted on fish and invertebrate CPUE at APE and two reference areas, contrasting CPUE from the months while construction was occurring to the same months during the baseline time period. Separate analyses were conducted for the two construction phases. Suitable CPUE data sets (predominantly non-zero catch for the months included in the construction phase models) were available for the construction phase I and phase II time periods for black sea bass, little skate, summer flounder, windowpane, and longfin squid.

Benthivore and piscivore assemblage composition was also examined among areas between the baseline and each of the construction time periods using separate two-factor PERMANOVA tests. Data were treated as described above for the multivariate tests of operation effects.

Regional Context

The NEFSC trawl survey is conducted in the fall (September and October) and spring (March to May) to determine the seasonal distribution, relative abundance, and community composition of demersal fish and invertebrates on the continental shelf. Temporal variability in the BIWF survey biomass data for these same months for the APE and the average of reference areas (REF) was compared to that of the NEFSC trawl survey conducted in Strata 3020 and 3450 (INSPIRE, 2021), which had comparable depths (23-44 m) to the BIWF survey and are located to the southwest and northeast of Block Island, respectively. Temporal trends in biomass between surveys were plotted for the fall (September and October) and spring (March to May) sampling events for each year as the residual catch, which is the difference between the seasonal CPUE and the overall average CPUE within a survey. Spearman's rank correlation coefficients were used to examine the similarity in temporal trends among surveys and locations (NEFSC, APE, and REF). The number of tows in each season ranged from 2 to 6 at APE, 4 to 12 at the reference areas, and 4 to 6 for the NEFSC survey. Species that were consistently sampled in both surveys include black sea bass, butterfish (*Peprilus triacanthus*), little skate, longfin squid, silver hake, spiny dogfish, summer flounder, windowpane, winter flounder, and winter skate.

Effect Sizes

In this paper, the magnitudes of spatial-temporal interaction effects for select species are summarized between the APE and each reference area, as well as between the two reference areas. The measured effect sizes provide real-world context for what level of change may be reasonable to target when planning future OSW monitoring studies of these fish and invertebrate species. Note that results are conditional on the sampling design and modeling approach used in this study. However, the sampling frequency for this study (i.e. monthly trawl samples over seven years) is sufficient to allow subsampling of the dataset to estimate variance and measurable effect sizes for alternative study designs (e.g. seasonal sampling).

The effect of primary interest in this study is the spatial-temporal interaction effect, i.e, the ratio of temporal (baseline vs. operation) change at a reference area relative to the temporal change at the APE. The magnitude of this contrast for the seven species tested between the APE and each of the two reference areas (totaling 14 contrasts) was summarized (i.e. range, median, mean, 25th, and 75th percentiles). The magnitude of this contrast between just the two reference areas was also calculated for each species to represent the level of natural variability that is present in the region, or what may constitute an ecologically meaningful effect size for these species.

Results

The target sampling intensity was achieved in nearly all months with the exception of three missed trawls in July 2014 and three missed trawls in November 2015 due to net damage. In July 2019, a large catch of spiny dogfish collected at APE required tripping the net, therefore this catch was lost.

Physical and biological parameters

Seasonal bottom water temperatures were similar across the seven years of monitoring (Supplementary Figure S1). Winter temperatures ranged from approximately 2 to 8°C, with the lowest temperatures occurring in 2015. Monthly average salinity ranged from approximately 31.0 to 33.5 ppt and DO concentrations were well above levels associated with hypoxic conditions, with monthly averages ranging from approximately 7.5 to 11.5 mg/L. There was a strong linear relationship between temperature and DO (Pearson's correlation coefficient -0.72, df $= 427$, $p < 0.001$). The linear regression of DO on temperature was used to estimate 22 missing DO values for inclusion in the catch models; two DO outliers (> 14.6 mg/L) were excluded from the regression analysis.

A total of 663 970 individual fish representing 61 species were collected in the seven years of the BIWF demersal trawl survey (Supplementary Appendix S2). Within each year, the five most abundant species accounted for 75%–93% of the total catch. Butterfish, little skate, and scup, were among the five most abundant species each year, whereas winter skate (5 years), Atlantic herring (4 years), spiny dogfish (2 years), silver hake (2 years), and northern sea robin (1 year) were less consistently among the most abundant species. At all areas, total fish abundances were highest in the first two years of sampling and were strongly influenced by large catches of schooling species such as butterfish and Atlantic herring, which accounted for over 74% of the annual catch for each of those years. A total of 113 752 invertebrates representing 29 taxa were collected, with longfin squid accounting for approximately 52% of all invertebrates (Supplementary Appendix S3). Other abundant invertebrates include Jonah crab (*Cancer borealis*), rock crab (*Cancer irroratus*), sand dollars (*Echinarachnius parma*), and sea scallops (*Placopecten magellanicus*).

Operation effects

The focus of this paper is on the measurable effects of the wind farm, hence the 90CIs and figures are provided in text for statistically significant ($\alpha = 0.10$) BACI interactions. The magnitude and precision of BACI interactions that were not statistically significant are also informative; these are provided along with estimates of the temporal and spatial contrasts in Supplementary Materials (Appendices S4 and S5; Figures S2 through S4).

Black sea bass, little skate, windowpane, and winter flounder exhibited statistically significant spatial-temporal
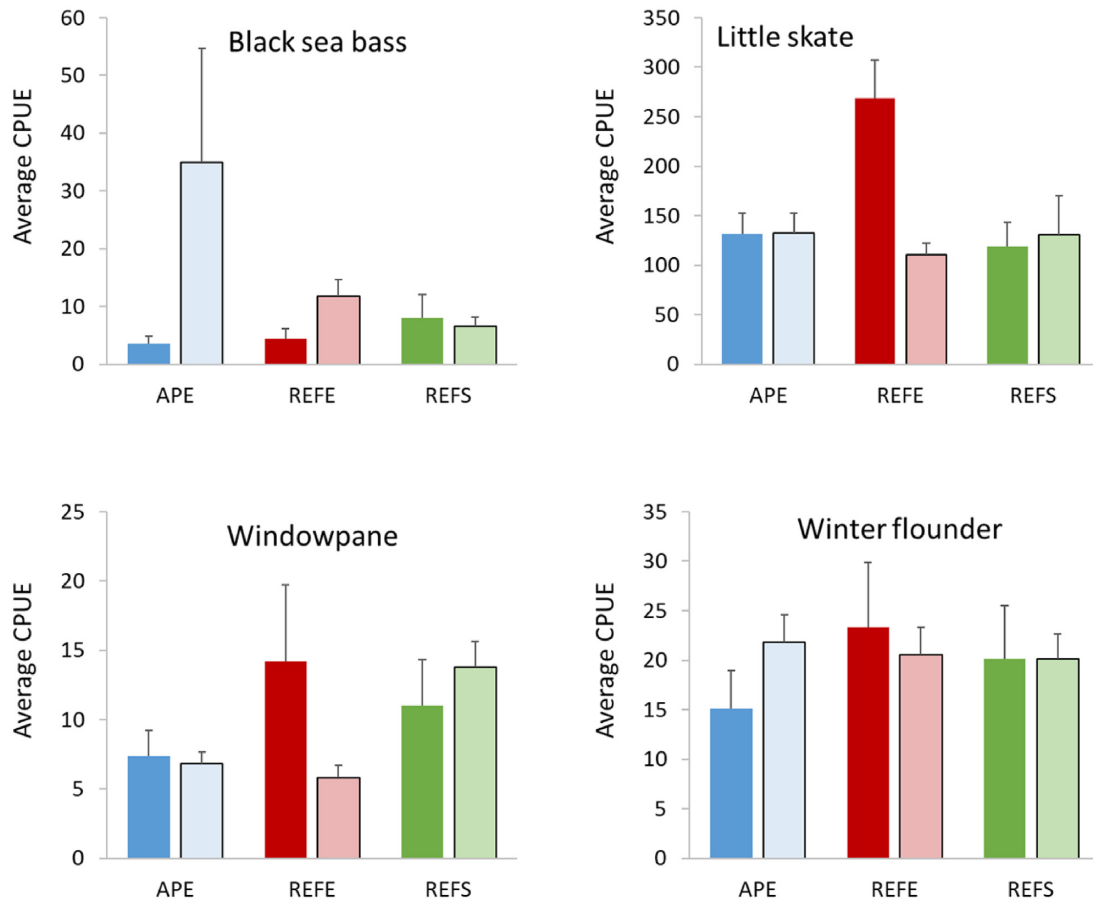
Figure 2. Average CPUE (monthly average abundance per tow) with standard error of black sea bass, little skate, windowpane, and winter flounder in each survey area for the baseline (October 2012 through September 2014) and operation (October 2016 through September 2019) time periods (shaded dark and light, respectively).

interactions between the APE and one of the reference areas (not necessarily the same one for each species), with a greater temporal increase or smaller temporal decrease in catch at the APE compared to the reference area. For instance, black sea bass CPUE increased by nearly an order of magnitude at APE between the baseline and operation time periods and decreased slightly at REFS (Figure 2). The estimated temporal ratio at REFS was 77% lower (90CI: −92%, −36%) than that at APE, indicating a higher proportional increase in CPUE at APE relative to REFS. Black sea bass CPUE increased approximately 289% between time periods at REFE (Figure 2; 90CI: +69%, +807%, Supplementary Appendix S4). Little skate CPUE decreased approximately 69% at REFE between the baseline and operation time periods and remained relatively constant at APE (Figure 2). The estimated temporal ratio at REFE was 56% lower (90CI: −73%, −29%) than the estimated temporal ratio at APE, indicating a higher proportional decrease in CPUE at REFE relative to APE. Summer flounder CPUE was approximately two- to three-times higher at REFS than at APE during the baseline (90CI: +11%, +244%) and operation time periods (90CI: +126%, +450%) (Supplementary Appendix S4 and Figure S2). Windowpane CPUE decreased approximately 61% at REFE and remained relatively constant at APE between the baseline and operation time periods (Figure 2), with an estimated temporal ratio at REFE that was 50% lower (90CI: −70%, −15%) than the estimated temporal ratio at APE, indicating a higher propor-

tional decrease in CPUE at REFE relative APE. Winter flounder CPUE at APE increased approximately 62% between the baseline and the operation time periods, whereas CPUE decreased slightly at REFE (Figure 2). The estimated temporal ratio at REFE was 60% lower (90CI: −76%, −32%) than the estimated temporal ratio at APE, indicating a higher proportional increase in CPUE at APE relative to the change at REFE.. Winter skate CPUE remained relatively constant at APE, increased slightly at REFS, and decreased at REFE between the baseline and operation time periods (Figure S2), while models that accounted for temperature and DO indicated that standardized catch values decreased from 33% to 64% across the three areas (Supplementary Appendix S4). Longfin squid CPUE decreased between the baseline and operation time periods approximately 32% at the APE and 44% at REFS (Figure S2).

Across all species, the BACI contrasts between the APE and REFE indicated that the APE had a smaller proportional temporal decrease or larger increase in CPUE than REFE for all species examined except summer flounder (Supplementary Appendix S4). The direction of the BACI contrasts between the APE and REFS varied across species (positive BACI contrasts were estimated for summer flounder, windowpane, and winter skate; negative contrasts were estimated for black seabass, little skate, winter flounder, and longfin squid).

Benthivore and piscivore assemblage compositions did not exhibit statistically significant ($\alpha = 0.05$) BACI contrasts in
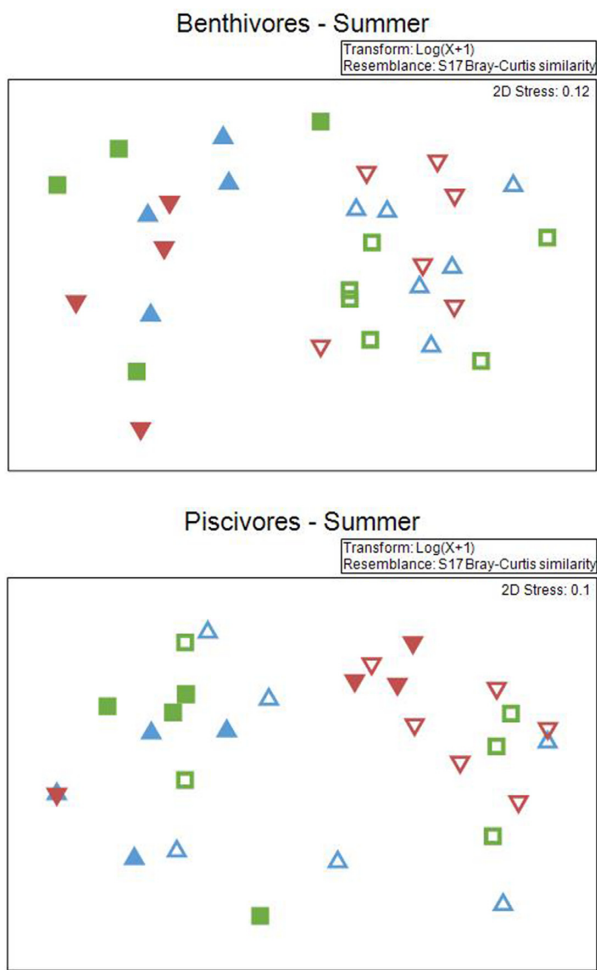
Benthivores - Summer

Piscivores - Summer

Figure 3. Non-metric multidimensional scaling plots depicting summer benthivore (top) and piscivore (bottom) fish assemblage dissimilarities among areas; APE (blue), REFE (red), and REFS (green) for the baseline and operation (solid and open symbols, respectively) time periods.

any season (Supplementary Appendix S5). Benthivore assemblage composition exhibited strong temporal differences in the winter (F = 6.72, p = 0.001, df = 1 and 42) and summer (F = 30.02, p = 0.001, df = 1 and 18). A strong difference in assemblage composition was apparent in the spring across areas (F = 4.60, p = 0.001, df = 2 and 29. Temporal differences in winter benthivore assemblage composition involved higher Atlantic herring, winter skate, and little skate CPUE during the baseline time period (SIMPER; Supplementary Appendix S6). Spring benthivore assemblage composition differences among areas reflected higher winter skate and little skate CPUE at REFS (SIMPER; Supplementary Appendix S6). The clearest temporal difference in benthivore assemblage composition occurred during the summer (Figure 3), when baseline CPUE of little skate and winter skate were higher and CPUE of northern sea robin and scup were lower than observed during the operation time period. Piscivore assemblage composition differed temporally and spatially. For example, fall piscivore assemblage composition differed between time periods (F = 3.65, p = 0.014, df = 1 and 30), due in part to higher CPUE of spiny dogfish, silver hake, and summer flounder during the operation time period (SIMPER). Spring spatial differences in assemblage composition (F = 5.48, p < 0.001,

df = 2 and 29) were due in part to higher CPUE of silver hake at REFE, spiny dogfish at APE, and summer flounder at REFS. Summer piscivore assemblages differed by time period (F = 7.87, p = 0.002, df = 1 and 18) and area (F = 3.03, p = 0.024, df = 2 and 18, Figure 3), with higher silver hake, summer flounder, and spiny dogfish CPUE during the operation time period. Silver hake and summer flounder CPUE were highest at REFE (SIMPER).

Construction effects
Black sea bass CPUE increased approximately 200% or more between baseline and the construction phase I time period (July 2015 through October 2015) in all areas (Supplementary Figure S3). Little skate CPUE increased at APE and REFS between the baseline and construction phase I time periods with a higher increase at REFS (Figure 4); the estimated temporal ratio at REFS was 143% higher (90CI: +36%, +333%) than the estimated temporal ratio at APE. Summer flounder CPUE increased between the baseline and construction phase I time periods at APE and decreased slightly at REFE (Figure 4), such that the estimated temporal ratio at REFE that was 80% lower (90CI: −93%, −45%) than the estimated temporal ratio at APE. Summer flounder CPUE at REFS also increased dramatically between time periods (90CI: +173%, +1036%, Supplementary Appendix S4; Figure 4). Windowpane CPUE were higher during the construction phase I time period in all areas (Figure 4) with more than a 260% increase at both APE and REFS and approximately 10% increase at REFE, yielding a statistically significant BACI interaction between REFE and APE. The estimated temporal ratio of windowpane CPUE at REFE was 50% lower (90CI: −70%, −15%) than the estimated temporal ratio at APE. Winter flounder had only relatively small changes in CPUE both temporally and spatially. Winter skate CPUE at REFS were higher than APE during both time periods, and CPUE at REFS more than doubled during the construction phase I time period compared to baseline (Supplementary Figure S3). Longfin squid CPUE decreased from approximately 43% to 90% between time periods among the three areas, with a statistically significant interaction involving REFS, whereby the estimated temporal ratio of CPUE at REFS was 70% lower (90CI: −88%, −24%) than the estimated temporal ratio at APE (Figure 4).

During the construction phase II time period (April 2016 through September 2016), black sea bass CPUE increased approximately 320% over baseline in the reference areas and 480% in the APE (Supplementary Figure S4). The estimated temporal ratio in little skate CPUE at APE statistically differed from the temporal ratios at REFE and at REFS, although in different directions (Figure 5). Little skate APE CPUE stayed relatively constant, whereas REFE experienced a decline, with a temporal ratio at REFE that was 47% lower (90CI: −70%, −8%) than the temporal ratio at APE. The REFS experienced a large increase in CPUE, resulting in an estimated temporal ratio at REFS that was 111% higher (90CI: +28%, +273%) than the temporal ratio at APE. Summer flounder CPUE was relatively constant in all areas between the baseline and the construction phase II time period (Supplementary Figure S4). Windowpane CPUE was more than 160% higher during the construction phase II time period in REFE and remained relatively constant at APE and REFS (Supplementary Figure S4). Winter flounder CPUE was relatively constant at REFE, and markedly higher during the construction phase II time period at REFS (212% increase) and the APE (73% increase)
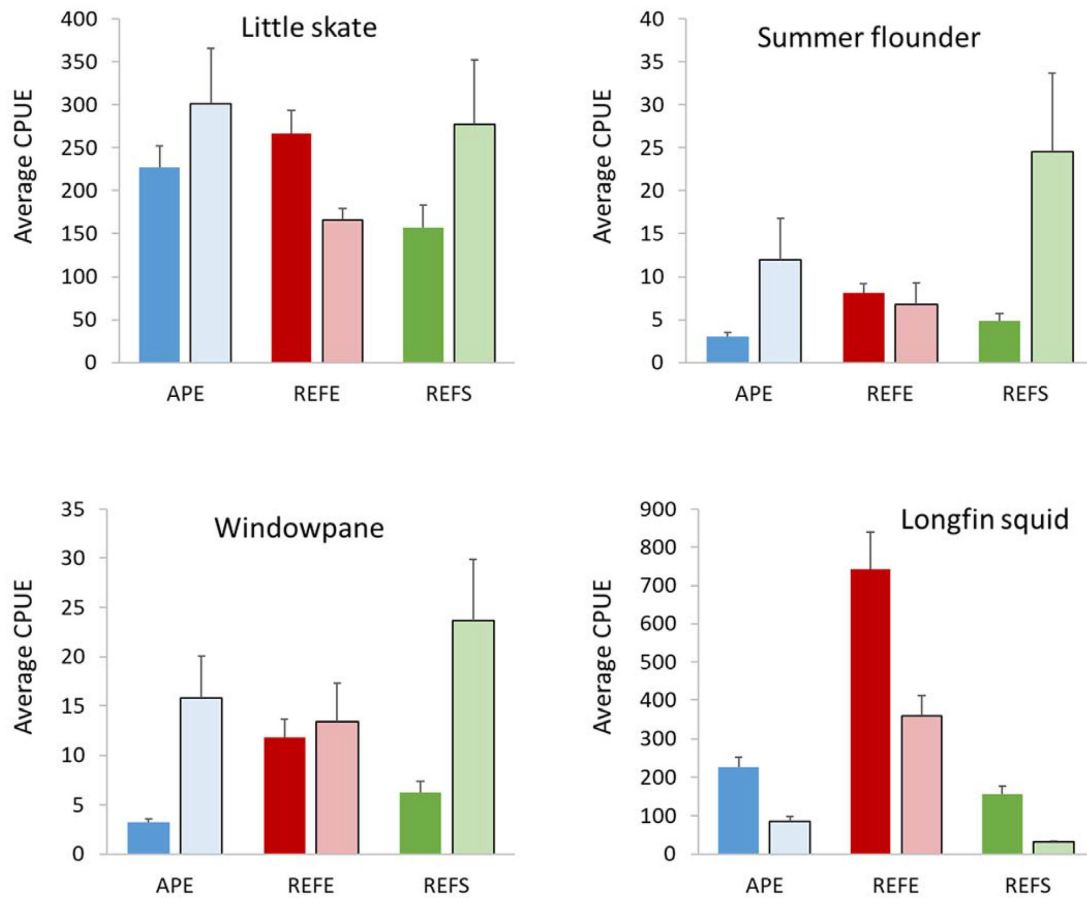
Figure 4. Average CPUE with standard error of little skate, summer flounder, windowpane, and longfin squid in each survey area for the baseline (July 2013 through October 2013; July 2014 through October 2014) and construction phase I (July 2015 through October 2015) time periods (shaded dark and light, respectively).

(Supplementary Figure S4). Winter skate CPUE decreased at APE and REFE, and increased at REFS. The BACI interaction with REFS estimated the temporal ratio of winter skate CPUE at REFS to be 162% higher (90CI: +1%, +565%) than the temporal ratio at APE (Figure 5). Longfin squid CPUE increased between time periods at APE and REFE and decreased at REFS, with a statistically significant interaction involving REFS, whereby the estimated temporal ratio of CPUE at REFS was 68% lower (90CI: −89%, −13%) than the temporal ratio at APE (Figure 5).

Benthivore and piscivore assemblages did not show a statistically detectable effect of either phase of wind farm construction (Supplementary Appendix S7). Temporal changes were evident between baseline and construction phase I time periods for both trophic groups. Spatial and temporal changes in CPUE of some benthivores contributing to these dissimilarities and not analyzed using GLMs include higher baseline CPUE of Atlantic herring (Figure 6), which were not observed during construction phase I, and decreased scup CPUE (approximately 30%) between baseline and construction phase I (Supplementary Appendix S7). Between the baseline and construction phase II time period Atlantic herring CPUE declined approximately 90%, while scup CPUE increased nearly 1800% and northern sea robin increased nearly 130% (Figure 6, Supplementary Appendix S7). Large catches of spiny dogfish occurred at APE during both phases of construction (Figure 6), contributing to higher average CPUE at

APE and during the construction time period I (Supplemental Appendix S7).

Regional Context

Temporal trends in CPUE (kg/tow) from 2012 through 2019 were compared between the BIWF monitoring survey and the NEFSC trawl survey to examine whether local trends at BIWF were reflected in regional observations. High seasonal variation in biomass for most species dominated long-term temporal trends over the seven-year study period (Supplementary Figure S5). For instance, in both surveys, black sea bass biomass typically was high in the fall and low in the spring (Spearman's $r_s = 0.52$ [NEFSC and APE] and $r_s = 0.51$ [NEFSC and REF]), and the BIWF survey had lower seasonal catches during the initial two years of sampling compared to latter years, a trend that was not as apparent in the NEFSC survey (Figure 7). Seasonal variation in fish biomass was similar between surveys for little skate, longfin squid, summer flounder, winter flounder, and winter skate (Supplementary Figure S5). Longfin squid biomass also exhibited strong seasonal variation in both surveys, with peaks in the fall (Figure 7) and there was strong synchrony among regional surveys (Spearman's $r_s = 0.82$ [NEFSC and APE] and $r_s = 0.92$ [NEFSC and REF]). Winter flounder exhibited the reverse seasonal variation in biomass, exhibiting synchrony between surveys (Spearman's $r_s = 0.46$ [NEFSC and APE] and $r_s = 0.52$ [NEFSC and REF]) and peaks in the spring.
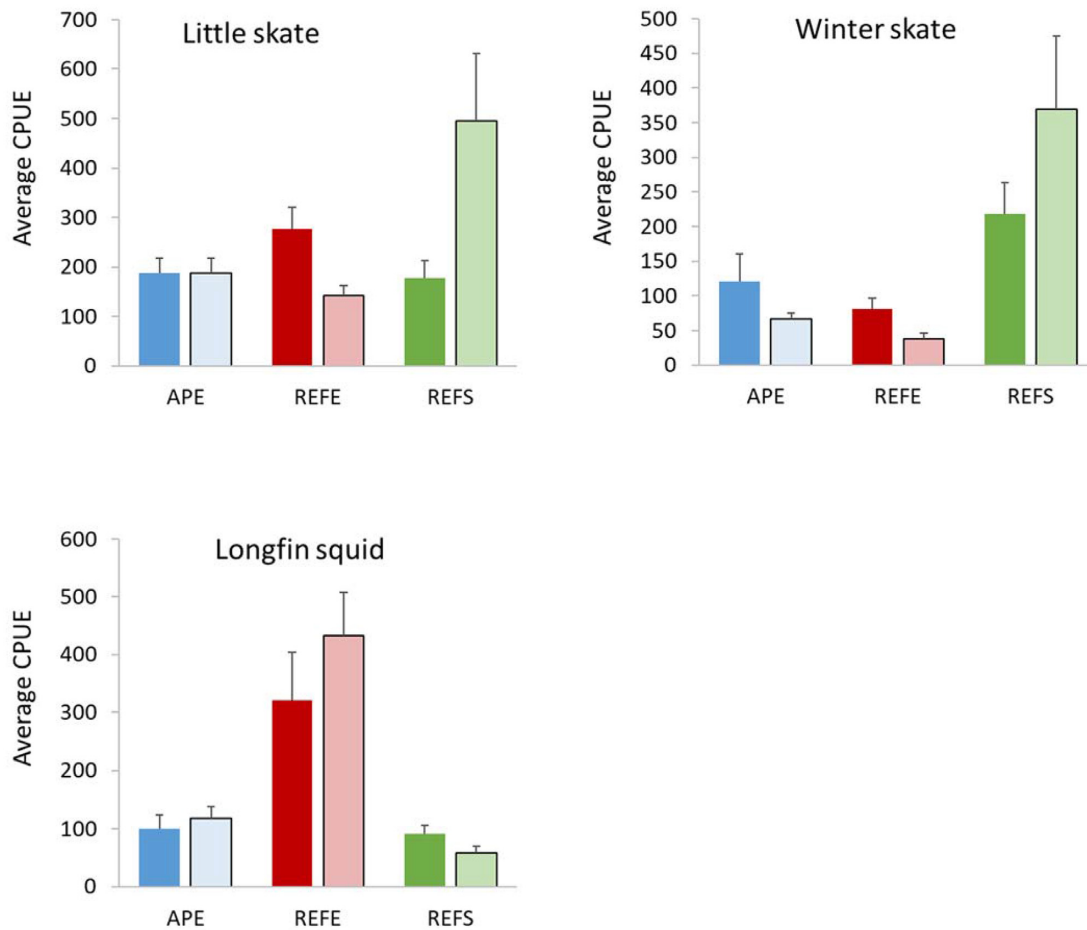
Figure 5. Average CPUE with standard error of little skate, winter skate, and longfin squid in each survey area for the baseline (April 2013 through September 2013; April 2014 through September 2014) and construction phase II (April 2016 through September 2016) time periods (shaded dark and light, respectively).

Effect sizes

Ten of the 14 contrasts indicated that CPUE increased at APE relative to reference areas between the baseline and operation time periods (Table 1). Only four of the 14 baseline-to-operation contrasts resulted in effect sizes that indicated a relative decline in CPUE at the APE and none of these contrasts were statistically significant ($\alpha = 0.10$). The median interaction effect size was small (-26%), equivalent to a 35% temporal increase in CPUE at APE relative to a numerically stable reference area (Table 1). Four of the 14 models identified statistically significant effects, with the significant interaction effect size values ranging from -77% to -50% (approximately a 335% to 100% temporal increase in CPUE at APE relative to a numerically stable reference area). Statistically significant changes in catch, therefore, were limited to large effect sizes, i.e. large temporal changes were required to yield a significant result. Across the six numerically dominant fish species, the spatial-temporal interaction effect size between the two reference areas, which approximates a background level of change, ranged from a 67% to 170% increase in one reference relative to the other (equivalently, a 40% to 63% decrease in CPUE at the second reference area relative to the first). Longfin squid showed relative stability between reference areas with approximately a 3% increase, or 3% decrease, in one area relative to the other.

Discussion

Demersal fish and invertebrate CPUE varied spatially between the APE and two reference areas and temporally between baseline and operation time periods, however interactions indicating reduced CPUE at the APE during wind farm operation were not apparent. The CPUE of several fish species were higher near the wind farm during the operation time period relative to the reference areas, providing evidence for an artificial reef effect (Degraer *et al.*, 2020). For example, black sea bass CPUEs were statistically higher during the operation period near the wind farm relative to a reference area, reflecting the structure-oriented behavior of this species. Black sea bass were observed near the BIWF turbine foundations in diver-based photographic transects (HDR, 2020), are targeted near the turbine foundations by recreational fishermen (Smythe *et al.*, 2021) and increased approximately ten-fold in CPUE in trawls conducted at APE over the reference areas in the first two years of wind farm operation. Black sea bass inhabit rocky habitat and reefs (Steimle and Zetlin, 2000; Fabrizio *et al.*, 2013) and also are attracted to artificial reefs in the region (Harrison and Rousseau, 2020). The increase in black sea bass CPUE at the wind farm occurred during a period of increasing biomass throughout the range of the stock (NEFSC, 2020). Atlantic cod CPUE also were higher near the wind farm after turbine installation. Cod are targeted by recre-
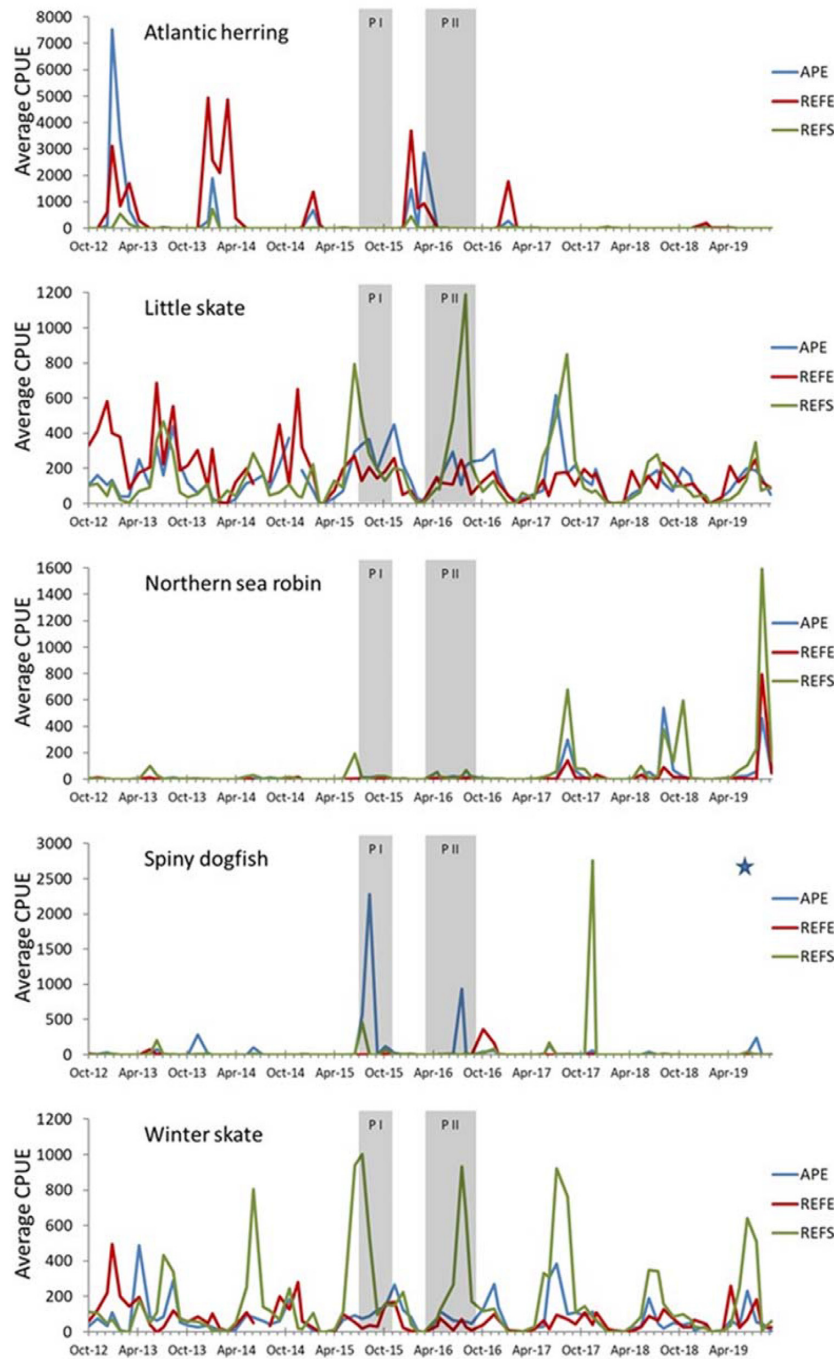
Figure 6. Average CPUE (catch/tow) for select species by project area across the seven-year study period. Gray bars depict the timing of construction phase I (P I) and phase II (P II). The star on the spiny dogfish graph represents a catch at APE that was too large to bring onboard the vessel.

ational fishermen at BIWF as they use underwater structures as refuge and foraging habitat (Page *et al.*, 2007; Fernandez *et al.*, 2008). Cod are attracted to the foundations of offshore wind turbines in the Netherlands (van Hal *et al.*, 2017), the Belgian part of the North Sea (Degraer *et al.*, 2012; Reubens *et al.*, 2013a, 2013c), and Sweden (Bergstrom *et al.*, 2013), and may benefit energetically from access to complex habitat that provides more access to shelter and higher prey availability (Schwartzbach *et al.*, 2020).

Temporal trends in relative abundances of schooling species such as Atlantic herring, scup, and butterfish (collectively sometimes called forage fish) reflected regional trends and did not indicate an effect of wind farm operation. These species were common in the BIWF demersal trawl survey and are important prey for commercially important pelagic species such as bluefish, striped bass, tuna, and shark (Buckel *et al.*, 1999; Chase, 2002; Link *et al.*, 2002). Atlantic herring CPUE declined throughout the survey period in all areas (Figure 6) consistent with a regional decline that led to an adjustment to Atlantic herring fishery catch limits by the New England Fishery Management Council (NEFSC, 2018; NEFMC, 2019). Butterfish CPUE also declined (Supplementary Appendix S2) and
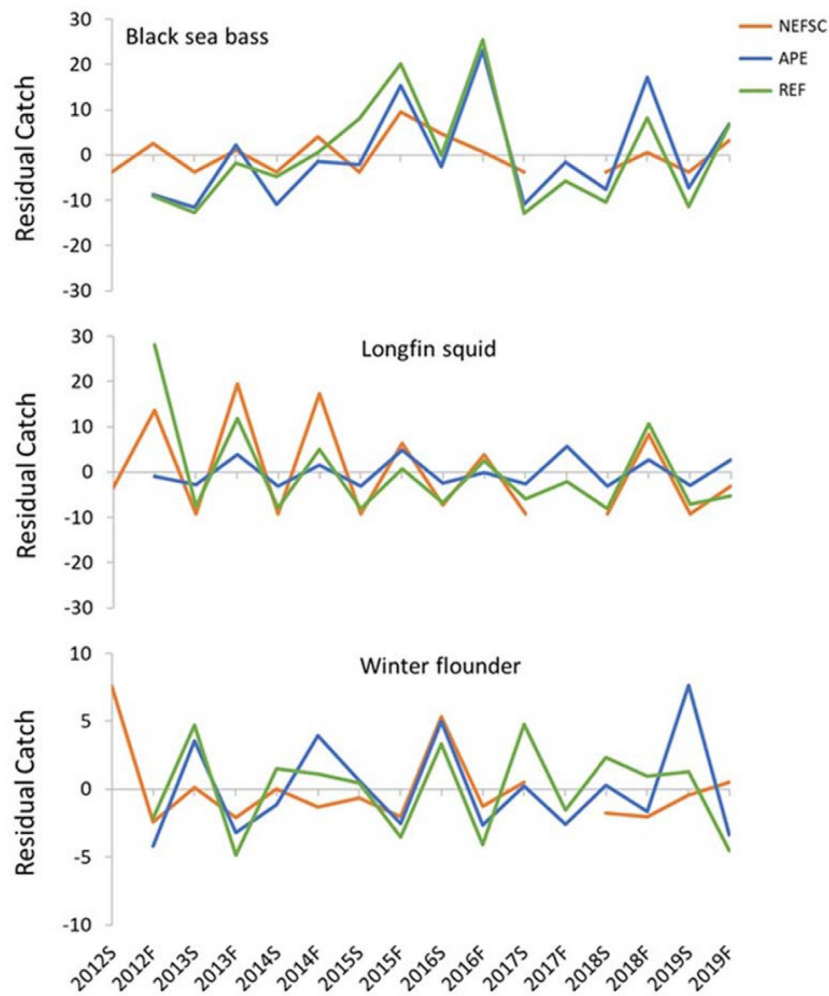
Figure 7. Temporal trends in catches of select species collected in the BIWF demersal trawl survey near the wind farm (APE) at the two reference areas (REF), and in the Northeast Fisheries Science Center (NEFSC) biannual bottom trawl survey in strata 3020 and 3450. Residual catch is the difference between the seasonal CPUE and the overall average CPUE within each survey.

Table 1. Observed unstandardized effect size (ES) values estimated from the BIWF species models contrasting baseline and operation abundance ratios between each reference area and the APE for the seven species examined. The second row converts each effect size to the relative % change at the APE, assuming that abundances at the reference area stay constant over time. Percentiles range from the minimum (Min) to maximum (Max). The wind farm area is the Area of Potential Effect (APE).

	Min	25th Percentile	Median	Mean	75th Percentile	Max
Observed ES	−77%	−48%	−26%	−20%	+3%	+83%
ES = Effect Size calculated as [(Reference Operation/Reference Baseline)/(APE Operation/APE Baseline) −1] x 100.						
ES converted to % Change at APE	+335%	+92%	+35%	+25%	−3%	−45%
Assume the Reference area stays constant (Operation/Baseline = 1), then temporal % Change at APE = ((1/(ES/100 + 1))−1) x 100.						

although the NOAA Fisheries 2018 butterfish stock assessment indicated it is not overfished, there is a concern that recruitment has declined in recent years (Adams, 2018). Scup CPUE increased throughout the survey period, consistent with increasing commercial and recreational landings in Southern New England since the early 2000s (ASMFC, 2015). Examinations of fish by trophic categories further identified temporal trends for some less abundant species, without an indication of a wind farm effect. For instance, higher northern sea robin CPUE during the operation time period may reflect a shift in distribution to deeper, colder areas from a warm-

ing Narragansett Bay where abundances are declining (Innes-Gold *et al.*, 2020).

Statistically significant interactions indicative of potential impacts were limited to little skate and winter skate at the wind farm compared to REFS, which may represent avoidance of construction activity in preference for REFS. However, the pronounced seasonal peaks in little skate and winter skate CPUEs at REFS during construction also occurred during the operation time period, and during the baseline period for winter skate (Figure 6), and therefore, may reflect seasonal use of favored habitat at fine spatial scales. Higher squid CPUE

during the baseline time period compared to the construction phase I time period that included pile driving are consistent with regional trends of lower commercial catches of squid during 2015 (Hendrickson, 2017), although fishery-dependent catch rates are additionally influenced by weather, economics, quotas, and regulations. High spiny dogfish catches at APE occurred during both phases of construction, with another high catch at REFS in the fall of 2017, and a tremendous catch at APE in July 2019 that was too large to be brought onboard (Figure 6). Spiny dogfish are voracious predators that consume commercially important prey, such as Atlantic cod, Atlantic herring, squid, butterfish, and Atlantic mackerel (Sagarese *et al.*, 2016). Their distribution and abundance are linked to that of their prey (Sagarese *et al.*, 2014) and they were captured in seabed images taken at BIWF (HDR, 2020). Their large-scale, migratory movements and schooling behavior can lead to large variability in trawl survey catch rates that complicate stock assessments (Frisk *et al.*, 2011; Sagarese *et al.*, 2015) and similarly, interpretations of potential wind farm impacts. The possibility that spiny dogfish may be attracted to the wind farm, both during construction and operation periods if prey species are more abundant, may contribute to the periodic high spiny dogfish catches.

In a period of environmental change, it is important to distinguish potential wind farm impacts on fish and invertebrates from underlying shifts in distributions that are associated with other factors. Range shifts to the north for winter flounder (Able *et al.*, 2014; Bell *et al.*, 2014), summer flounder (Perretti and Thorson, 2019; Bell *et al.*, 2014), and black sea bass (Miller *et al.*, 2016; McBride *et al.*, 2018) are well documented and in the case of winter flounder and black sea bass, are linked to warming oceanic temperatures. Fish recruitment on the northeast continental shelf is linked to regime shifts in copepod communities, with durations of high and low recruitment lasting decades (Perretti *et al.*, 2017). In addition, northeastern shifts in fish and macroinvertebrate distributions may be in response to a similar shift in copepod distributions (Friedland *et al.*, 2018). Given this background, it is likely that fish and invertebrate assemblages at BIWF will change over the multi-decade life of the project, which makes it essential to compare monitoring results to regional trends in fish and invertebrate distributions that are established through long-term monitoring. The BIWF and NEFSC trawl survey data exhibited strong seasonal variation that likely reflects the cross-shelf migratory nature of the species examined. For instance, the offshore fall migrations of adult black sea bass (Fabrizio *et al.*, 2013) and longfin squid (Buresch *et al.*, 2006) were evident as fall biomass peaks in both surveys. Spring peaks in winter flounder biomass also are consistent with cross-shelf movement as winter flounder in southern New England leave estuaries and inshore areas in the spring as water temperatures increase (DeCelles and Cadrin, 2011). The seasonal synchrony between the surveys suggests proximity to the wind farm did not disrupt cross-shelf movements. Future monitoring, if seasonal, may not fully capture population trends as fish and invertebrate migrations shift temporally in response to thermal changes (Langan *et al.*, 2021).

The BIWF demersal trawl survey fulfilled the purpose of documenting the seasonal relative abundance of demersal fish and invertebrates during baseline, construction, and operation time periods through a collaboration among the commercial/recreational fishing, scientific, and resource management communities. A demersal trawl was used in this study for com-parability to long-term regional trends and because sediment disturbances during construction and operational vibrations may be more likely to affect bottom-dwelling species. Trawls capture a wide range of species and size classes, making them a preferred multispecies sampling method. Relative decreases in fish and invertebrate abundances during wind farm operation were neither statistically (Table S4) nor substantively (e.g. Figure 6; and INSPIRE, 2021) evident. However, statistically significant results for fish were limited to large effect sizes, demonstrating that large temporal changes in relative abundance were required to yield a statistically significant result, even though considerable sampling effort was expended over seven years. Additionally, results were not always consistent for contrasts between APE and each reference area, further illustrating fine-scale spatial variation in fish and invertebrate distributions. Sampling included 497 tows that collected approximately three-quarters of a million fish and invertebrates. Moving forward, studies that use fish abundances as a metric of OSW effects should specify biologically meaningful effect sizes to inform the design of the study to characterize that level of change with sufficient statistical power or precision (ROSA, 2021; Mapstone, 1995). Presently, thresholds associated with biologically meaningful effect sizes have not been established for fish and invertebrates in relation to offshore infrastructure in the US. Prior to the BIWF demersal trawl study, sufficient historical data were not available for the area to conduct power analyses for planning purposes. Presently, estimates of the magnitude of effects observed at BIWF with confidence intervals are being used to inform study designs that measure the effects of offshore wind on the northeast Atlantic continental shelf. Additional work is needed to identify critical effect sizes for fisheries monitoring and the BIWF dataset can contribute to this effort (e.g. using methods presented in Arciszewski and Munkittrick, 2015; Munkittrick *et al.*, 2009; Nakagawa and Cuthill, 2007; Mapstone, 1995; Osenberg *et al.*, 1994). The basic monitoring of spatial and temporal abundance trends surrounding wind farm installation and operation can be enhanced at future wind farms when paired with targeted research that addresses potential mechanisms of effects (*sensu* Degraer *et al.*, 2019; Popper *et al.*, 2021) or less extractive methodologies (e.g. acoustic telemetry, acoustic monitoring with drones, passive acoustic monitoring, optical methods, sonar, spatial modeling, eDNA).

Supplementary Materials

Supplementary materials are available at the *ICESJMS* online version of the manuscript and include the full output of the GLMs for all species and impact phases (Appendix S1), species lists of fish and invertebrates (Appendices S2 and S3), median and 90CI estimates for all statistical contrasts estimated from the GLMs (Appendix S4), results of multivariate tests (Appendices S5–S7), bottom water temperature (Figure S1), graphs of observed CPUE values for species with non-significant BACI interactions (Figures S2–S4) and graphs comparing biomass of select species in the BIWF survey to a regional survey over the seven-year study period (Figure S5).

Funding

Author contributions

Data availability

The data underlying this article were provided by Deepwater Wind Block Island.

Conflicts of Interest

The authors have no conflicts of interest to declare.

Acknowledgements

References

Able, K. W., Grothues, T. M., Morson, J. M., and Coleman, K. E. 2014. Temporal variation in winter flounder recruitment at the southern margin of their range: is the decline due to increasing temperatures? ICES Journal of Marine Science, 71: 2186–2197.

Adams, C. F. 2018. Butterfish 2017 stock assessment update. US Dept Commer, Northeast Fish Sci Cent Ref Doc. 18-05 31 p. Available from: http://www.nefsc.noaa.gov/publications/

Anderson, M. J., Gorley, R. N., and Clarke, K. R. 2008. PERMANOVA+ for PRIMER: Guide to Software and Statistical Methods. Plymouth: PRIMER-E Ltd.

Andersson, M. H., and Ohman, M. C. 2010. Fish and sessile assemblages associated with wind-turbine constructions in the Baltic Sea. Marine and Freshwater Research, 61: 642–650.

Arciszewski, T. J., and Munkittrick, K. R. 2015. Development of an adaptive monitoring framework for long-term programs: an example using indicators of fish health. Integrated Environmental Assessment and Management, 11: 701–718.

Atlantic States Marine Fisheries Commission (ASMFC). 2015. Scup benchmark stock assessment for 2015. 323 p. Arlington, VA.

Bailey, H., Brookes, K. L., and Thompson, P. M. 2014. Assessing environmental impacts of offshore wind farms: lessons learned and recommendations for the future. Aquatic Biosystems, 10: 1–13.

Bell, R. J., Hare, J. A., Manderson, J. P., and Richardson, D. E. 2014. Externally driven changes in the abundance of summer and winter flounder. ICES Journal of Marine Science, 71: 2416–2428.

Bergstrom, L., Sundqvist, F., and Bergstrom, U. 2013. Effects of an offshore wind farm on temporal and spatial patterns in the demersal fish community. Marine Ecology Progress Series, 485: 199–210.

Blanchard, J. L., Maxwell, D. L., and Jennings, S. 2008. Power of monitoring surveys to detect abundance trends in depleted populations: the effects of density-dependent habitat use, patchiness, and climate change. ICES Journal of Marine Science, 65: 111–120.

Bonzek, C. F., Gartland, J., Gauthier, D. J., and Latour, R. J. 2017. Northeast Area Monitoring and Assessment Program (NEAMAP) Data collection and analysis in support of single and multispecies stock assessments in the Mid-Atlantic: Northeast Area Monitoring and Assessment Program Near Shore Trawl Survey. Virginia Institute of Marine Science, College of William and Mary. Available from: https://doi.org/10.25773/7206-KM61.

Buckel, J. A., Fogarty, M. J., and Conover, D. O. 1999. Foraging habits of bluefish, *Pomatomus saltatrix*, on the U.S. east coast continental shelf. Fishery Bulletin, 97: 758–775.

Buresch, K. C., Gerlach, G., and Hanlon, R. T. 2006. Multiple genetic stocks of longfin squid *Loligo pealeii* in the NW Atlantic: stocks segregate inshore in summer, but aggregate offshore in winter. Marine Ecology Progress Series, 310: 263–270.

Burnham, K. P., and Anderson, D. R. 2002. Model selection and multimodel inference: a practical information-theoretic approach. 2nd ed. New York, Springer-Verlag.

Chase, B. C. 2002. Differences in diet of Atlantic bluefin tuna (*Thunnus thynnus*) at five seasonal feeding grounds on the New England continental shelf. Fishery Bulletin, 100: 168–180.

Clarke, K. R., Gorley, R. N., Somerfield, P. J., and Warwick, R. M. 2014. Change in marine communities: an approach to statistical analysis and interpretation. 2nd edition. PRIMER-E, Plymouth, United Kingdom.

DeCelles, G., and Cadrin, S. X. 2011. An interdisciplinary assessment of winter flounder stock structure. Journal of Northwest Atlantic Fishery Science, 43: 103–120.

S. Degraer, R. Brabant, and B. Rumes (Eds.) 2012. Offshore wind farms in the Belgian part of the North Sea: Heading for an understanding of environmental impacts. Royal Belgian Institute of Natural Sciences, Management Unit of the North Sea Mathematical Models, Marine ecosystem management unit. 155 pp. + annexes.

S. Degraer, R. Brabant, B. Rumes, and L. Vigin (Eds). 2018. Environmental Impacts of Offshore Wind Farms in the Belgian Part of the North Sea: Assessing and Managing Effect Spheres of Influence. Royal Belgian Institute of Natural Sciences, OD Natural Environment, Marine Ecology and Management: Brussels. 136pp.

S. Degraer, R. Brabant, B. Rumes, and L. Vigin (Eds). 2019. Environmental Impacts of Offshore Wind Farms in the Belgian Part of the North Sea: Marking a Decade of Monitoring, Research and Innovation. Brussels: Royal Belgian Institute of Natural Sciences, OD Natural Environment, Marine Ecology and Management, 134p.

Degraer, S., Carey, D. A., Coolen, J. W. P., Hutchison, Z. L., Kerckhof, F., Rumes, B., and Vanaverbeke, J. 2020. Offshore wind farm artificial reefs affect ecosystem structure and functioning: a synthesis. Oceanography, 33: 48–57.

Elliott, J., Smith, K., Gallien, D. R., and Khan, A. 2017. Observing Cable Laying and Particle Settlement During the Construction of the Block Island Wind Farm. Final Report to the U.S. Department of the Interior, Bureau of Ocean Energy Management, Office of Renewable Energy Programs. OCS Study BOEM 2017-027. 225pp.

Fabrizio, M. C., Manderson, J. P., and Pessutti, J. P. 2013. Habitat associations and dispersal of black sea bass from a mid-Atlantic Bight reef. Marine Ecology Progress Series, 482: 241–253.

Fernandez, T. V., D'Anna, G., Badalamenti, F., and Perez-Ruzafa., A. 2008. Habitat connectivity as a factor affecting fish assemblages in temperate reefs. Aquatic Biology, 1: 239–248.

Friedland, K. D., McManus, M. C., Morse, R. E., and Link, J. S. 2018. Event scale and persistent drivers of fish and macroinvertebrate distributions on the Northeast US Shelf. – ICES Journal of Marine Science, doi:10.1093/icesjms/fsy167.

Frisk, M. G., Duplisea, D. E., and Trenkel, V. M. 2011. Exploring the abundance-occupancy relationships for the Georges Bank finfish and shellfish community from 1963 to 2006. Ecological Applications, 21: 227–240.

Guarinello, M. L., and Carey, D. A. 2020. Multi-modal approach for benthic impact assessments in moraine habitats: a case study at the Block Island Wind Farm. Estuaries and Coasts doi.org/10.1007/s12237-020-00818-w.

Guida, V., Drohan, A., Welch, H., McHenry, J., Johnson, D., Kentner, V., Brink, J. *et al.* 2017. Habitat Mapping and Assessment of Northeast Wind Energy Areas. Sterling, VA: US Department of the Interior,

Bureau of Ocean Energy Management. OCS Study BOEM 2017-088. 312p.

Harrison, S., and Rousseau, M. 2020. Comparison of artificial and natural reef productivity in Nantucket Sound, MA, USA. Estuaries and Coasts, 43: 2092–2105.

HDR. 2020. Benthic and Epifaunal Monitoring During Wind Turbine Installation and Operation at the Block Island Wind Farm, Rhode Island – Project Report. Final Report to the U.S. Department of the Interior, Bureau of Ocean Energy Management, Office of Renewable Energy Programs. OCS Study BOEM 2020-044. Volume 1: 263 pp.; Volume 2: 380pp.

Hendrickson, L. C. 2017. Longfin inshore squid (Doryteuthis (Amerigo) pealeii) stock assessment for 2017. U.S. National Marine Fisheries Service, https://www.fisheries.noaa.gov/species/longfin-squid.

Hutchison, Z. L., Secor, D. H., and Gill, A. B. 2020. The interaction between resource species and electromagnetic fields associated with electricity production by offshore wind farms. Oceanography, 33: 96–107.

Innes-Gold, A., Heinichen, M., Gorospe, K., Truesdale, C., Collie, J., and Humphries, A. 2020. Modeling 25 years of food web changes in Narragansett Bay (USA) as a tool for ecosystem-based management. Marine Ecology Progress Series, 654: 17–33.

INSPIRE Environmental. 2021. Block Island Wind Farm Demersal Fish Trawl Survey, Final Synthesis Report – Years 1 to 7, October 2012 through September 2019. Prepared by INSPIRE Environmental, Newport, RI for Deepwater Wind Block Island, LLC, Providence, RI. 113pp.

Jackman, S. 2020. Classes and Methods for R Developed in the Political Science Computational Laboratory. United States Studies Centre, University of Sydney. Sydney, New South Wales, Australia. R package version 1.5.5. URL Available from: https://github.com/atahk/pscl/

LaFrance, M., Shumchenia, E., King, J., Pockalny, R., Oakley, B., Pratt, S., and Boothroyd, J. 2010. Benthic habitat distribution and subsurface geology selected sites from the Rhode Island Ocean special area management study area. Ocean Special Area Management Plan Volume 2, Appendix 4. Available from: https://seagrant.gso.uri.edu/oceansamp/pdf/appendix/04-LaFrance_et_al_SAMPreport.pdf.

Langan, J. A., Puggioni, G., Oviatt, C. A., Henderson, M. E., and Collie, J. S. 2021. Climate alters the migration phenology of coastal marine species. Marine Ecology Progress Series 660: 1–18.

Langhamer, O., Holand, H., and Rosenqvist, G. 2016. Effects of an offshore wind farm (OWF) on the common shore crab *Carcinus maenas*: tagging pilot experiments in the lillgrund offshore wind farm (Sweden). Plos One 11: e0165096.

Leonard, S. B., Stenberg, C., and Stottrup, J. 2011. Effects of the horns Rev 1 offshore wind farm on fish communities: follow-up seven years after construction. DTU Aqua Report No 246-2011. 99pp.

Lindeboom, H. J., Kouwenhoven, H. J., Bergman, M. J. N., Bouma, S., Brasseur, S., Daan, S., Fijn, R. C. *et al.* 2011. Short-term ecological effects of an offshore wind farm in the Dutch coastal zone; a compilation. Environmental Research Letters, 6: 1–13.

Lindén, A., and Mäntyniemi, S. 2011. Using the negative binomial distribution to model overdispersion in ecological count data. Ecology, 92: 1414–1421.

Link, J. S., Garrison, L. P., and Almeida, F. P. 2002. Ecological interactions between elasmobranchs and groundfish species on the northeastern U.S. continental shelf. I. Evaluating predation. North American Journal of Fisheries Management, 22: 550–562.

Lipsky, A., Moura, S., Kenney, A., and Bellavance, R. 2016. Addressing interactions between fisheries and offshore wind development: the block island wind farm. 16pp.

Maar, M., Bolding, K., Petersen, J. K., Hansen, J. L. S., and Timmermann, K. 2009. Local effects of blue mussels around turbine foundations in an ecosystem model of Nysted off-shore wind farm, Denmark. Journal of Sea Research, 62: 159–174.

Malek, A. J., Collie, J. S., and Gartland, J. 2014. Fine-scale spatial patterns in the demersal fish and invertebrate community in a northwest Atlantic ecosystem. Estuarine Coastal and Shelf Science, 147: 1–10.

Malek, A. J., Collie, J. S., and Taylor, D. L. 2016. Trophic structure of a coastal fish community determined with diet and stable isotope analyses. Journal of Fish Biology, 89: 1513–1536.

Mapstone, B. D. 1995. Scalable decision rules for environmental impact studies: effect size, type I, and type II errors. Ecological Applications, 5: 401–410.

McBride, R. S., Tweedie, M. K., and Oliveira, K. 2018. Reproduction, first-year growth, and expansion of spawning and nursery grounds of black sea bass (*Centropristis striata*) into a warming Gulf of Maine. Fishery Bulletin, 116: 323–336.

Miller, A. S., Shepherd, G. R., and Fratantoni, P. S. 2016. Offshore habitat preference of overwintering juvenile and adult black sea bass, *Centropristis striata*, and the relationship to year-class success. Plos One 11: e0147627.

Munkittrick, K. R., Arens, C. J., Lowell, R. B., and Kaminski, G. P. 2009. A review of potential methods of determining critical effect size for designing environmental monitoring programs. Environmental Toxicology and Chemistry, 28: 1361–1371.

Nakagawa, S., and Cuthill, I. C. 2007. Effect size, confidence interval and statistical significance: a practical guide for biologists. Biological Reviews, 82: 591–605.

National Academies of Sciences, Engineering, and Medicine (NASEM). 2017. Atlantic Offshore Renewable Energy Development and Fisheries: Proceedings of a Workshop—in Brief. Washington, DC: The National Academies Press. doi: https://doi.org/10.17226/25062.

New England Fisheries Management Council (NEFMC). 2019. NMFS Final Rule – February 8, 2019. (accessed June 2019). Available from: https://www.nefmc.org/library/atlantic-herring-in-season-adjustments.

Northeast Fisheries Science Center (NEFSC). 2018. 65th Northeast regional stock assessment workshop (65th SAW) assessment summary report. US Dept Commer, Northeast Fish Sci Cent Ref Doc. 18-08; 38 p. Available from: http://www.nefsc.noaa. gov/publications/.

Northeast Fisheries Science Center (NEFSC) 2020. Operational assessment of the black sea bass, scup, bluefish, and monkfish stocks, updated through 2018. NEFSC Ref Doc 20-01: 160 p. Available from http://www.nefsc.noaa.gov/publications/.

Osenberg, C. W., Schmitt, R. J., Holbrook, S. J., Abu-Saba, K. E., and Flegal, A. R. 1994. Detection of environmental impacts: Natural variability, effect size, and power analysis. Ecological Applications, 4: 16–30.

Page, H. M., Dugan, J. E., Schroeder, D. M., Nishimoto, M. M., Love, M. S., and Hoesterey, J. C. 2007. Trophic links and condition of a temperate reef fish: comparisons among offshore oil platform and natural reef habitats. Marine Ecology Progress Series, 344: 245–256.

Perretti, C. T., and Thorson, J. T. 2019. Spatio-temporal dynamics of summer flounder (*Paralichthys dentatus*) on the Northeast US shelf. Fisheries Research, 215: 62–68.

Perretti, C. T., Fogarty, M. J., Friedland, K. D., Hare, J. A., Lucey, S. M., McBride, R. S., Miller, T. J. *et al.* 2017. Regime shifts in fish recruitment on the Northeast US continental shelf. Marine Ecology Progress Series, 574: 1–11.

Popper, A., Hice-Dunton, L., Williams, K., and Jenkins, E. 2021. Sound and vibration effects on fishes and aquatic invertebrates workgroup report (DRAFT). State of the science workshop on wildlife and offshore wind energy 2020: cumulative impacts. Prepared for New York State Energy Research and Development Authority. May 19, 2021. Available at: https://www.nyetwg.com/2020-workgroups.

Popper, A. N., and Hawkins, A. D. 2019. An overview of fish bioacoustics and the impacts of anthropogenic sounds on fishes. Journal of Fish Biology, 94: 692–713.

R Core Team. 2020. R: A language and environment for statistical computing. R Foundation for Statistical Computing, Vienna, Austria. Available from: http://www.R-project.org/.

Reubens, J. T., Braeckman, U., Vanaverbeke, J., Van Colen, C., Degraer, S., and Vincx, M. 2013a. Aggregation at windmill artificial reefs: CPUE of Atlantic cod (*Gadus morhua*) and pouting (*Trisopterus luscus*) at different habitats in the Belgian part of the North Sea. Fisheries Research, 139: 28–34.

Reubens, J. T., Vandendriessche, S., Zenner, A. N., Degraer, S., and Vincx, M. 2013b. Offshore wind farms as productive sites or ecological traps for gadoid fishes? – impact on growth, condition index and diet composition. Marine Environmental Research, 90: 66–74.

Reubens, J. T., Pasotti, F., Degraer, S., and Vincx, M. 2013c. Residency, site fidelity and habitat use of Atlantic cod (*Gadus morhua*) at an offshore wind farm using acoustic telemetry. Marine Environmental Research, 90: 128–135.

ROSA. 2021. Offshore wind project monitoring framework and guidelines. March 2021. Responsible Offshore Science Alliance.

Sagarese, S. R., Frisk, M. G., Cerrato, R. M., Sosebee, K. A., Musick, J. A., and Rago, P. J. 2014. Application of generalized additive models to examine ontogenetic and seasonal distributions of Spiny Dogfish (*Squalus acanthias*) in the northeast (US) shelf large marine ecosystem. Canadian Journal of Fisheries and Aquatic Sciences, 71: 847–877.

Sagarese, S. R., Frisk, M. G., Cerrato, R. M., Sosebee, K. A., Musick, J. A., and Rago, P. J. 2015. Spatiotemporal overlap of spiny dogfish (*Squalus acanthias*) and commercial fisheries in the northeast U.S. shelf large marine ecosystem. Fishery Bulletin, 113: 101–120.

Sagarese, S. R., Frisk, M. G., Cerrato, R. M., Sosebee, K. A., Musick, J. A., and Rago, P. J. 2016. Diel variations in survey catch rates and survey catchability of spiny dogfish and their pelagic prey in the Northeast U.S. Continental Shelf Marine Ecosystem. Marine and Coastal Fisheries: Dynamics, Management, and Ecosystem Science, 8: 244–262.

Schad, D. J., Vasishth, S., Hohenstein, S., and Kliegl, R. 2020. How to capitalize on a priori contrasts in linear (mixed) models: a tutorial. Journal of Memory and Language 110: 104038.

Schwartzbach, A., Behrens, J. W., and Svendsen, J. C. 2020. Atlantic cod *Gadus morhua* save energy on stone reefs: implications for the attraction versus production debate in relation to reefs. Marine Ecology Progress Series, 635: 81–87.

Secor, D., O'Brien, M., Rothermel, E., Wiernicki, C., and Bailey, H. 2020. Movement and habitat selection by migratory fishes within the Maryland Wind Energy Area and adjacent reference sites. Sterling (VA): U.S. Department of the Interior, Bureau of Ocean Energy Management, Office of Renewable Energy Programs. OCS Study BOEM 2020-030. 109p.

Seltman, H. J. 2018. Experimental Design and Analysis. Carnegie Mellon University. 428pp. Available from: http://www.stat.cmu.edu/~hseltman/309/Book/Book.pdf.

Smith, E. P., Orvos, D. R., and Cairns, J. 1993. Impact assessment using the before-after-control-impact (BACI) model: concerns and comments. Canadian Journal of Fisheries and Aquatic Sciences, 50: 627–637.

Smith, S. J. 1996. Analysis of data from bottom trawl surveys. Northwest Atlantic Fisheries Organization (NAFO) Scientific Council Studies, 28: 25- 53.

Smythe, T., Bidwell, D., and Tyler, G. 2021. Optimistic with reservations: the impacts of the United States' first offshore wind farm on the recreational fishing experience. Marine Policy, 127: 104440.

Steimle, F. W., and Zetlin, C. 2000. Reef habitats in the middle Atlantic Bight: abundance, distribution, associated biological communities, and fishery resource use. Marine Fisheries Review, 62: 24–42.

Stenberg, C., Stottrup, J. G., van Deurs, M., Berg, C. W., Dinesen, G. E., Mosegaard, H., Grome, T. M. *et al.* 2015. Long-term effects of an offshore wind farm in the North Sea on fish communities. Marine Ecology Progress Series, 528: 257–265.

Taormina, B., Bald, J., Want, A., Thouzeau, G., Lejart, M., Desroy, N., and Carlier, A. 2018. A review of potential impacts of submarine power cables on the marine environment: knowledge gaps, recommendations and future directions. Renewable and Sustainable Energy Reviews, 96: 380–391.

Tofighi, D., and MacKinnon, D. P. 2016. Monte carlo confidence intervals for complex functions of indirect effects. Structural Equation Modeling: A Multidisciplinary Journal, 23: 194–205.

Tougaard, J., Hermannsen, L., and Madsen, P. T. 2020. How loud is the underwater noise from operating offshore wind turbines? Journal of the Acoustical Society of America, 148: 2885–2893.

Underwood, A.J. 1992. Beyond BACI: the detection of environmental impacts on populations in the real, but variable, world. Journal of Experimental Marine Biology and Ecology, 161: 145–178.

van Deurs, M., Grome, T. M., Kaspersen, M., Jensen, H., Stenberg, C., Sorensen, T. K., Stottrup, J. *et al.* 2012. Short- and long-term effects of an offshore wind farm on three species of sandeel and their sand habitat. Marine Ecology Progress Series, 458: 169–180.

Vandendriessche, S., Derweduwen, J., and Hostens, K. 2015. Equivocal effects of offshore wind farms in Belgium on soft substrate epibenthos and fish assemblages. Hydrobiologia, 756: 19–35.

van Hal, R., Griffioen, A. B., and van Keeken, O. A. 2017. Changes in fish communities on a small spatial scale, an effect of increased habitat complexity by an offshore wind farm. Marine Environmental Research 126: 26–36.

Venables, W. N., and Ripley, B. D. 2002. Modern Applied Statistics with S. Fourth Edition. Springer, New York. ISBN 0-387-95457-0.

Ver Hoef, J. M., and Boveng, P. L. 2007. Quasi-poisson vs. negative binomial regression: how should we model overdispersed count data? Ecology, 88: 2766–2772.

Wahlberg, M., and Westerberg, H. 2005. Hearing in fish and their reactions to sounds from offshore wind farms. Marine Ecology Progress Series, 288: 295–309.

Walsh, H. J., and Guida, V. G. 2017. Spring occurrence of fish and macro-invertebrate assemblages near designated wind energy areas on the northeast U.S. continental shelf. Fishery Bulletin, 115: 437–450.

Wilber, D H., Brown, L., Griffin, M., DeCelles, G R., and Carey, D. A. 2022. Offshore wind farm effects on flounder and gadid dietary habits and condition on the northeastern US coast. Marine Ecology Progress Series, 683: 123-138.

Wolfson, A., van Blaricom, G., Davis, N., and Lewbel, G. S. 1979. The marine life of an offshore oil platform. Marine Ecology Progress Series, 1: 81–89.

Zeileis, A., and Hothorn, T. 2002. Diagnostic checking in regression relationships. R News 2: 7–10. Available from: https://CRAN,R-project.org/doc/Rnews/

Handling Editor: Michael Pol